High-Resolution Solid-State ^{13}C NMR Study of Chitosan and Its Salts with Acids: Conformational Characterization of Polymorphs and Helical Structures as Viewed from the Conformation-Dependent ^{13}C Chemical Shifts

Hazime Saitô* and Ryoko Tabeta

Biophysics Division, National Cancer Center Research Institute, Tsukiji 5-chome, Chuo-ku, Tokyo, Japan 104

Kozo Ogawa

Radiation Center of Osaka Prefecture, Shinke-cho, Sakai, Osaka, Japan 593.
Received October 1, 1986

ABSTRACT: We have recorded high-resolution solid-state ^{13}C NMR spectra of chitosan and its salts with 11 inorganic and organic acids. First, we noted that the ^{13}C NMR spectra of chitosans differ appreciably between preparations from shells of crab and shrimp, reflecting their polymorphs, "tendon chitosan" and "L-2", respectively. These spectral patterns were further converted to another spectral profile, in which the C-1 and C-4 peaks are substantially displaced, by annealing the chitosans in water at 200–222 °C. When chitosan salts were formed with inorganic or organic acids, the two types of helical structures resulting were easily distinguishable by their ^{13}C NMR spectra. The observation of singlets for the C-1 and C-4 carbons in the type I (HNO_3, $HClO_4$, HBr, HI, and CF_3COOH) salts of chitosan was satisfactorily interpreted in terms of the presence of the 2-fold helical conformation proposed previously. On the other hand, the doublet splitting of the C-1 carbon of the type II (HCl, H_2SO_4, H_3PO_4, HIO_4, and HCOOH) salts was ascribed to the presence of the 4-fold helix of dimeric units, rather than the 8-fold helix of monomeric residues, although the alternative model with two independent chains could not be completely ruled out.

Introduction

Chitosan is a polymer of β-(1→4)-linked 2-amino-2-deoxy-D-glucose residues which is easily derived by deacetylation of chitin and possesses remarkable ability to form complexes with heavy metal ions or salts with acids due to the presence of free amino groups in the repeating units.[1] This is the reason why, in recent years, much attention has been paid to the potential utilization of chitosan for collecting heavy metal ions or acids from industrial wastes. To gain insight into the stability of these salts and complexes, it is very important to clarify resulting conformational features of these complexes and salts in the solid state. In this connection, previous X-ray diffraction studies showed that a conformational change of chitosan accompanies the process of complex-formation or protonation.[2,3] In particular, two types of helical structures in chitosan salts were revealed by X-ray diffraction study: a 2-fold helical conformation similar to that of chitosan (HNO_3, HBr, and HI salts) and a left- or right-handed helix having eight residues in three turns or 4-fold helix of the dimer residues (HF, HCl, and H_2SO_4 salts).[3] It is expected that additional information about the molecular conformation could be obtained by solid-state ^{13}C NMR data as a complementary means to X-ray diffraction.

For this purpose, it has been demonstrated that the conformation-dependent ^{13}C chemical shifts of the C-1 and C-*X* carbon atoms of polysaccharides, which are next to the glycosidic linkages, vary appreciably (up to 8 ppm) with the torsion angles at the glycosidic linkages, C-1–O_{gly} (ϕ) and O_{gly}–C-*X* (ψ), respectively.[4,20] Thus, conformational features of cellulose,[7-15] chitin,[16,17] and (1→3)-β-D-[18-20] and (1→4)-α-D-glucans[5,6,21,22] have been analyzed by high-resolution solid-state ^{13}C NMR spectroscopy. In addition, conformational characterization utilizing the conformation-dependent ^{13}C chemical shifts has been extensively examined for other molecular systems including peptides, polypeptides, fibrous proteins, naturally occurring and synthetic ionophores, etc.[4,23]

In the present paper, we aim to clarify conformational features of various types of chitosans and chitosan salts with a variety of inorganic or organic acids, by means of high-resolution solid-state ^{13}C NMR spectroscopy.

Experimental Section

Materials. We used three kinds of chitosan preparations. Chitosan fiber (crab tendon chitosan) was prepared from a crab tendon chitin by deacetylation with saturated NaOH solution for 45 h at 100 °C, followed by washing with water and drying in air.[3] Chitosan powder from a crab shell of *Chionecetes opilio* O. Fabricius was kindly provided by Professor S. Hirano of Tottori University. Chitosan powder from a shrimp shell was supplied by Katokichi Co., Ltd., Kannonji, Kagawa, Japan. Annealed chitosan samples were prepared by heating either shrimp or crab chitosans in water at 200–220 °C in a closed bomb.[24]

Most of the chitosan salts were prepared from shrimp chitosan, since the resulting ^{13}C NMR spectra of the salts were the same for the three kinds of chitosans mentioned above. Chitosan salts with inorganic acids were prepared by immersing the shrimp chitosan in aqueous media containing 6 N inorganic acids for 15 min under vigorous stirring at ambient temperature.[3] Resulting chitosan salts were washed and dehydrated with an excess of isopropyl alcohol and were dried in air. A sample of annealed chitosan hydrochloride was prepared by heating the hydrochloride in 80% isopropyl alcohol at 160 °C in a sealed bomb, followed by washing with isopropyl alcohol.[3] Chitosan salts with organic acids (CF_3COOH, CH_3COOH, and HCOOH) were prepared by dissolving the shrimp chitosan in these acids, depositing onto a film of poly(vinylidene chloride), and drying the resulting film in vacuo at ambient temperature for over 5 h. The extent of salt formation was found to be greater than 90% from the ^{13}C NMR spectra, as described later. A chitin sample from crab shell used as a reference for the ^{13}C NMR spectra was purchased from Sigma Chemical Co.

Method. Single-contact 75.46-MHz ^{13}C CP-MAS (cross-polarization–magic angle spinning) NMR spectra were recorded on a Bruker CXP-300 spectrometer equipped with a CP-MAS accessory. Most of the solid samples were contained in an Andrew-Beams-type rotor machined from perdeuteriated poly(methyl methacrylate), and spectra were recorded with use of a Bruker z-32DR ^{13}C MAS probe. Some ^{13}C NMR spectra were recorded by employing a Bruker z-32DR-MAS-DB probe of a double air-

0024-9297/87/2220-2424$01.50/0

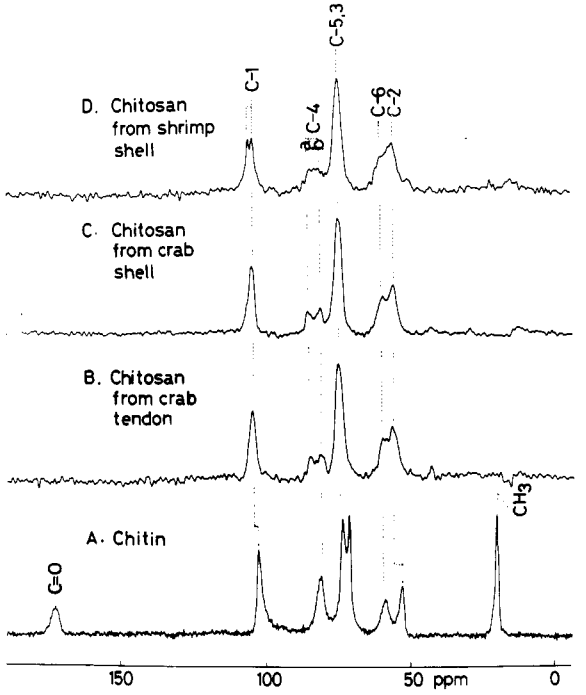

Figure 1. ^{13}C CP-MAS NMR spectra, 75.46 MHz, of chitin and of chitosan samples prepared from three different sources: (A) chitin; (B) crab tendon chitosan; (C) crab shell chitosan; (D) shrimp shell chitosan.

Table I
^{13}C Chemical Shifts of Chitosan from Various Sources (ppm from TMS)

	C-1	C-4	C-5,C-3	C-6	C-2
crab tendon	104.1	84.3, 80.9	74.6	59.8	56.6
crab shell	105.0	85.6, 81.2	75.5	60.3	56.4
shrimp shell	105.7, 104.3	84.5–80.3	75.0	60.9	56.8
annealed[a]	102.7	82.7	73.9	61.9	57.3

[a] Narrow peaks.

bearing type. In this case, samples were contained in a ceramic cylindrical rotor. The 90° pulse width was 5 μs and the repetition time was 4 s. The contact time for cross polarization was 1 ms. Spectra were usually accumulated 500–2000 times, depending on the type of probe. ^{13}C chemical shifts were calibrated indirectly from the signal of liquid benzene (128.5 ppm) and converted to the value from tetramethylsilane.

X-ray powder patterns of chitosans and their HCl salts were measured at room humidity (ca. 40% relative humidity) by a Rigaku Geigerflex X-ray diffractometer RAD-IIIA employing Ni-filtered Cu Kα radiation generated at 40 kV and 30 mA.

Results and Discussion

Polymorphs of Chitosans. So far, the following six polymorphs have been proposed for chitosan:[24-27] "tendon-chitosan",[25] "annealed",[24] "1-2", "L-2",[26] "form I", and "form II".[27] The single molecular chain in these polymorphs has always been observed to be extended 2-fold helical structures similar to chitin or common cellulose.[28] Therefore, it is of interest to know how the ^{13}C chemical shifts of chitosans are displaced by going from one polymorph to the other. We aim in this paper to examine ^{13}C NMR spectra of chitosans from various sources. In Figures 1 and 2, we illustrate 75.46-MHz ^{13}C CP-MAS NMR spectra of the crab tendon, crab shell, and shrimp shell chitosans as well as chitin and of annealed chitosans, respectively. Simultaneously, we recorded X-ray powder patterns of these samples as illustrated in Figure 3.

The ^{13}C NMR signals in Figures 1 and 2 were assigned, as shown in these figures and Table I, on the basis of the

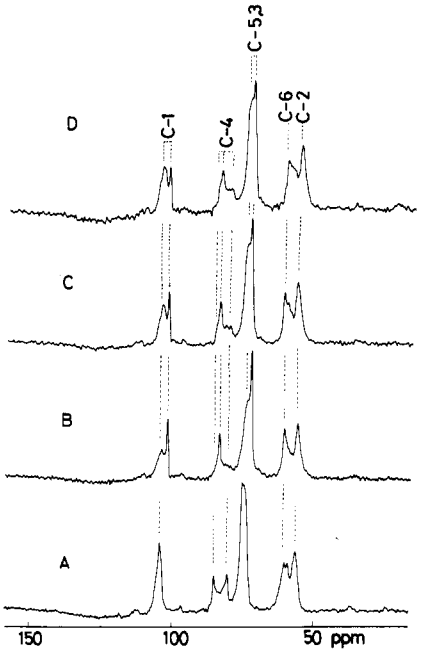

Figure 2. Variation of ^{13}C CP-MAS NMR spectra of chitosans with annealing: (A) untreated crab shell chitosan; (B) crab shell chitosan annealed at 220 °C; (C) crab shell chitosan annealed at 200 °C; (D) shrimp shell chitosan annealed at 220 °C.

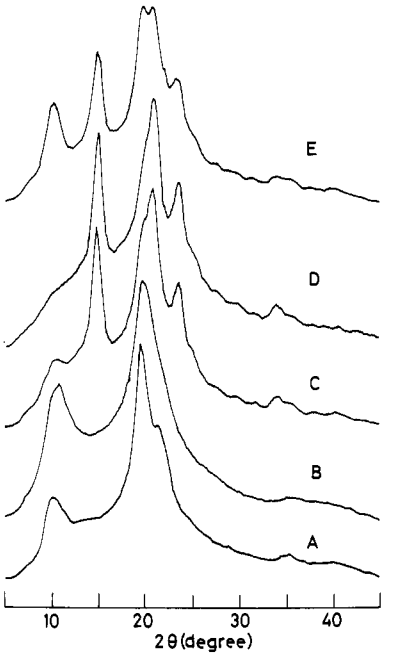

Figure 3. X-ray powder diffraction patterns of crab and shrimp shell chitosans and their annealed samples: (A) crab shell chitosan; (B) shrimp shell chitosan; (C) crab shell chitosan annealed at 200 °C; (D) crab shell chitosan annealed at 220 °C; (E) shrimp shell chitosan annealed at 220 °C.

peak assignments in the β-anomer of 2-amino-2-deoxy-D-glucopyranose[29] and the magnitude of displacement of peaks due to formation of a glycosidic linkage.[30] Apparently, there remains no appreciable amount of chitin in these chitosan samples, in view of the complete absence of the methyl and carbonyl signals arising from unreacted chitin (Figure 1A).[16,17]

Obviously, the ^{13}C NMR spectra of the crab shell chitosan is exactly the same as that of the well-oriented crab tendon chitosan (Figure 1B,C), because ^{13}C NMR spectra are generally insensitive to the manner of orientation of samples. Therefore, it is concluded that the crab shell chitosan assumes the structure of the "tendon chitosan"

polymorph.[24] This conclusion is further supported by the X-ray powder pattern of the crab shell chitosan (Figure 3A), which coincides with the fiber pattern of the crab tendon chitosan reported previously:[3] the peaks having lattice angle 2θ = 10.4°, 19.6°, and 21.4° correspond to the equatorial (200), (020), and (220) and (202) reflections of the tendon chitosan, respectively. As the most notable feature, the C-4 ^{13}C NMR signal of this polymorph appears as a doublet, the separation of which is 3.4–4.4 ppm (see Table I), but the C-1 ^{13}C NMR signal is a singlet. In contrast, the C-1 ^{13}C signal of shrimp chitosan (Figure 1D) is split into a doublet with a peak separation of 1.4 ppm, but the C-4 signal in this case appears as a plateau whose edges (C-4a and C-4b) correspond to the doublet peak of the crab chitosan. This finding suggests that the shrimp chitosan assumes a different conformation from that of the "tendon chitosan". In fact, the X-ray powder pattern of the shrimp chitosan (Figure 3B) gave a different pattern from that of the crab shell chitosan: the two peaks having lattice angles of 10.6° and 19.8° correspond to the respective equatorial (100) and (020) reflections of the L-2 polymorph of chitosan reported by Sakurai et al.[26]

As shown in Figure 2, the C-1 and C-4 ^{13}C NMR signals of the annealed chitosans are generally split into a pair of sharp and broad components, although the relative proportion of the sharp and broad components is considerably varied with the annealing temperature (Figure 2B,C) or the type of chitosan (Figure 2D). The sharp and broad components are clearly ascribable to the presence of the annealed and tendon chitosan polymorphs, respectively, because the peak positions of the latter coincide with those of the unannealed crab shell chitosan (Figure 2A). Therefore, these samples are considered as mixtures of these two polymorphs. Supporting this view, the X-ray powder patterns in Figure 3 show that the crab shell chitosan annealed at 220 °C coincides with the polymorph of annealed chitosan reported previously:[24] the peak having lattice angle of 15.1° corresponds to the (120) reflection; that of 20.9° to (200), (040), (102), and (020); that of 23.7° to (220) and (140) reflections. Again, the chitosan annealed at lower temperature, 200 °C, and the annealed shrimp chitosan are found to be mixtures of the above-mentioned two polymorphs (Figure 3C–E). As reported previously with the crab shell chitosan,[24] the extent of conversion from the "tendon chitosan" to annealed form depends upon the molecular weight of chitosan. Thus, the higher molecular weight chitosan did not show complete conversion to the annealed polymorph even at higher temperature because of the lower mobility of its polymer chains.

It is now clear that the C-1 and/or C-4 peaks of the tendon chitosan and L-2 polymorph of the shrimp chitosan are split into the doublets, whereas these signals were converted to the sharp singlet peaks in the annealed form. The observation of the latter spectral feature is in good agreement with that of chitin (Figure 1A)[16,17] and native cellulose (cellulose I)[7,8,13] which are known to adopt the extended helical conformations.[28] Darmon and Rudall[31] suggested that the lattice of tendon chitosan showed the same symmetry as the unit cell of α-chitin. If so, it is rather difficult to account for the doublet patterns of the C-1 and/or C-4 peaks in the tendon chitosan and L-2 polymorphs.

In this connection, it is worthwhile to recall that the C-1 and C-4 peaks of regenerated cellulose (cellulose II) gave peak splittings[7,10,11,14] (of equal peak intensities) as large as 2 and 1 ppm, respectively. The existence of two peaks for the C-1 and C-4 carbons was first interpreted in terms

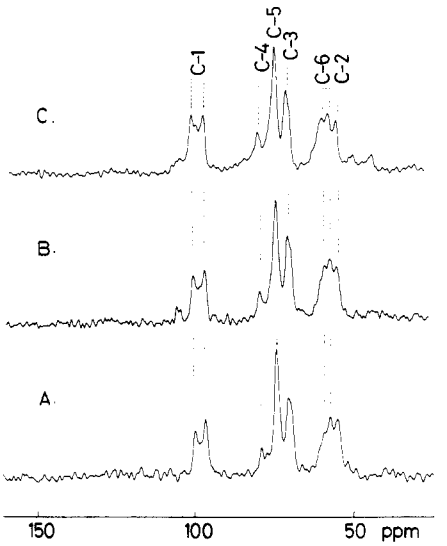

Figure 4. ^{13}C CP-MAS NMR spectra, 75.46 MHz, of chitosan HCl salts prepared from various chitosan samples: (A) crab tendon chitosan; (B) crab shell chitosan; (C) shrimp shell chitosan. The smaller peak(s) at 103–105 ppm could be ascribed to the C-1 peak of unreacted chitosan. The smaller peak at 44 ppm arose from carbon signal of rotor material.

of a nonequivalence of alternate glycosidic linkages (i.e., two sets of torsion angles) along the molecular chain.[7] This interpretation requires that dimeric cellobiose, rather than glucose, should be considered as the basic repeating unit of cellulose II. Instead, Dudley et al.[9] proposed, on the basis of comparison of the ^{13}C NMR spectra of cellulose II and cellulose oligomers, that cellulose II is made up of two independent chains (with different torsion angles). In a similar manner, VanderHart et al. proposed that the multiplicity in the C-1 and C-4 reflects the presence of more than two anhydroglucose residues per unit cell in the crystal.[10] Later, however, they proposed a model of two magnetically nonequivalent distinct crystal forms in the unit cell.[11] In addition, we previously noted that the C-1 peak of a number of (1→3)-β-D-glucans was split into a doublet with peak-separation as large as 1.6–2.1 ppm, when these samples were lyophilized from DMSO solution.[20] Thus, it is plausible that nonequivalence of two polymer chains of (1→3)-β-D-glucans was also created by the presence of hydrogen bonds with DMSO molecules (1:1 adduct as viewed from the ^{13}C NMR peak intensity).

Hence, it is likely that the observed multiplicity of the C-1 and C-4 ^{13}C NMR peaks in chitosan samples is explained by conformational nonequivalence of two independent chains caused by the presence of water molecules[32] loosely bound between the chitosan chains along the [010] direction. Then, it is natural to expect that the ^{13}C NMR pattern could be substantially modified when chitosan samples are completely dehydrated by annealing in water at temperatures of around 200 °C (annealed polymorph[24]). This is what we observed: the C-1 and C-4 ^{13}C NMR peaks are converted into the corresponding sharp singlet peaks by annealing at 220 °C (Figure 2B). Previous X-ray diffraction study as well as thermogravimetry and differential thermal analysis[24] showed that there is only a small difference in chain packing between the tendon chitosan and annealed polymorphs, except for the presence or absence of water molecules. Consequently, the observation of resulting singlet patterns in the C-1 and C-4 ^{13}C signals of annealed chitosan is consistent with the presence of a single 2-fold helix.

Helical Structures of Chitosan Salts. Figure 4 illustrates the ^{13}C CP-MAS NMR spectra of three kinds of

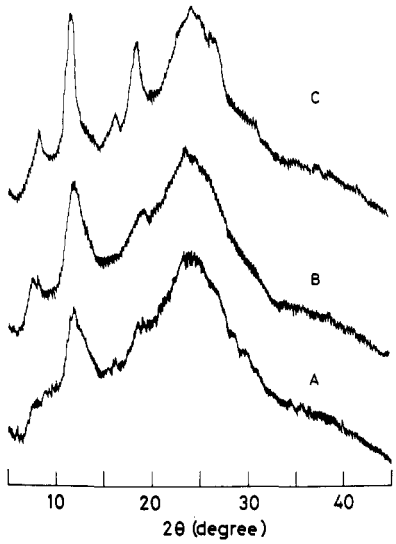

Figure 5. X-ray powder diffraction patterns of chitosan HCl salts and the effect of annealing: (A) crab shell chitosan HCl salt; (B) shrimp shell chitosan HCl salt; (C) crab shell chitosan HCl salt annealed at 160 °C.

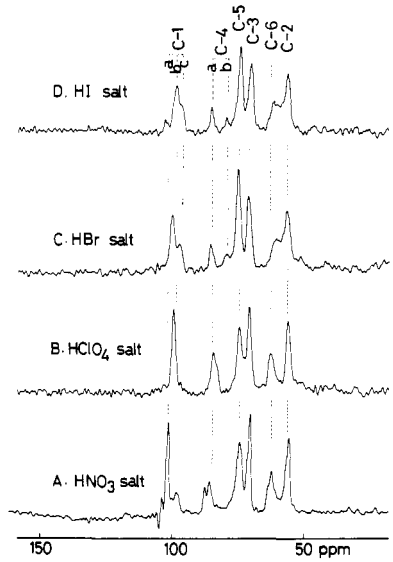

Figure 6. ^{13}C CP-MAS NMR spectra, 75.46 MHz, of type I (HNO_3, $HClO_4$, HBr, and HI) salts of chitosan.

chitosan HCl salts from the crab tendon, crab shell, and shrimp shell. Exactly the same spectral patterns were produced in spite of differences in polymorphs and the extent of orientation in the starting materials. In addition, we found that the X-ray powder pattern of the crab shell chitosan HCl salt was exactly the same as that of the shrimp chitosan HCl salt (Figure 5), although crystallinity of the former is higher than that of the latter. Therefore, we mainly used the shrimp chitosan as the starting material for salt formation in the present paper. Figures 6 and 7 illustrate the ^{13}C CP-MAS NMR spectra of chitosan salts with HNO_3, $HClO_4$, HBr, and HI (type I salts) and with HCl, H_2SO_4, H_3PO_4, and HIO_4 (type II salts), respectively. The presence of these two types of salts is readily shown by their characteristic NMR patterns.

To allow a quantitative comparison of peak intensities, it is essential to examine experimental conditions as referred to the following relaxation parameters: $T_{1\rho}$, the proton spin–lattice relaxation time in the rotating frame; T_{CH}, the cross polarization relaxation time; T_{1H}, the proton spin–lattice relaxation time. T_{CH} and $T_{1\rho}$ values were obtained by the initial exponential rise in intensity at

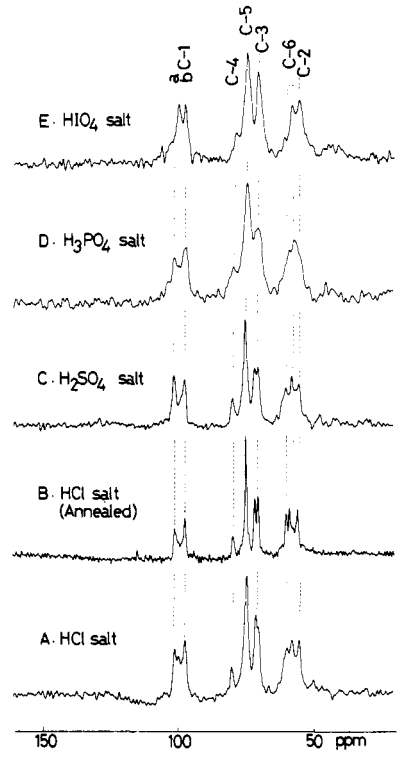

Figure 7. ^{13}C CP-MAS NMR spectra, 75.46 MHz, of type II (HCl, H_2SO_4, H_3PO_4, and HIO_4) salts. Annealed samples were prepared from shrimp chitosan HCl salt.

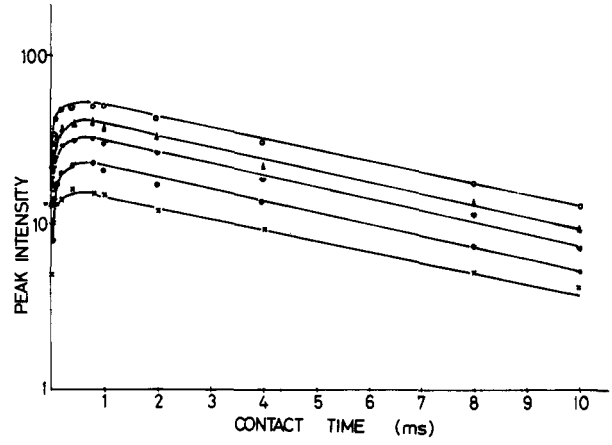

Figure 8. Plot of peak intensities of ^{13}C CP-MAS NMR of chitosan HCl salt vs. contact time: (●) C-1; (▽) C-2 (C-6); (△) C-3; (×) C-4; (○) C-5.

Table II
Relaxation Parameters of Typical Chitosan Salts (±15%)

samples		C-1	C-2	C-3	C-4	C-5	C-6
HCl salt	T_{CH}, μs	89	52[a]	62	45	90	52[a]
(type II)	$T_{1\rho}$, ms	6.2	6.2[a]	6.0	6.9	6.1	6.2[a]
	T_{1H}, s	0.40	0.48[a]	0.50	0.46	0.48	0.48[a]
HNO_3 salt	T_{CH}, ms	0.14	0.17	0.11	0.12	0.16	0.17
(type I)	$T_{1\rho}$, ms	9.8	7.6	9.3	7.3	6.2	6.1
	T_{1H}, s	0.87	0.57	0.66	0.70	0.64	0.54

[a] Treated as a single peak.

shorter contact time and the exponential decrease in intensity of longer contact time, respectively, in a plot of individual peak intensities as a function of the contact time,[33] as illustrated in Figure 8. The T_{1H} values were measured by the pulse sequence via ^{13}C CP-MAS,[34] in which the 180° pulse and variable delay time were inserted prior to standard cross polarization. Representative re-

Table III
Variety of Anions Leading to Either Type I or Type II Salts[a]

type I	type II	type I	type II
NO_3^-			$H_2PO_4^-$
ClO_4^-			IO_4^-
Br^-	(Br^-)	CF_3COO^-	
I^-	(I^-)	(CH_3COO^-)	CH_3COO^-
	Cl^-	($HCOO^-$)	$HCOO^-$
	HSO_4^-		

[a] Anions in parentheses lead to minor forms.

laxation data for the two typical kinds of salts, HCl and HNO_3 salts, are summarized in Table II. These relaxation data are in good agreement with those of a similar system recently published.[35] Consequently, it is concluded that the contact time of 1 ms used in this work is sufficient to allow complete cross polarization:[34]

$$T_{CH} \ll \text{contact time} \ll T_{1\rho}$$

In addition, a repetition time of 4 s is satisfactory, because the proton spin–lattice relaxation was complete during this time.

In Figure 9 we show the ^{13}C CP-MAS NMR spectra of chitosan salts (film samples) with some organic acids. The ^{13}C NMR signals for the methyl and/or carboxyl peaks from acids are clearly seen in CH_3COOH and HCOOH salts, but the carboxyl peak is somewhat obscured in the CF_3COOH salt. In general, the line widths of the ^{13}C NMR signals in these salts are much broader than those observed in the inorganic salts, since a drastic conformational change of chitosan might occur during dissolution in these organic acids. Nevertheless, the observed conformations, as concluded from the resulting ^{13}C NMR spectra, can be classified into either the above-mentioned type I form (CF_3COOH) or mixtures of the type I and II forms (CH_3COOH and HCOOH salts). We summarize the variety of anions leading to these two types of salts, as shown in Table III.

Type I Salts. The C-1 and C-4 peaks of HNO_3, $HClO_4$, and CF_3COOH salts gave respective singlet peaks, whereas those of HBr and HI, CH_3COOH and HCOOH salts showed additional minor peaks (C-1c and C-4b) besides the major peaks (C-1a and C-4a, respectively) arising from the type II salts as a minor component (see Figures 6, 7, and 9 and Table IV).[36] In the previous X-ray diffraction study,[3] the chitosan HNO_3 salt showed a sharp fiber pattern indicating high crystallinity. It is also suggested that chitosan keeps its 2-fold helical structure during formation of these salts and that this type of salt does not

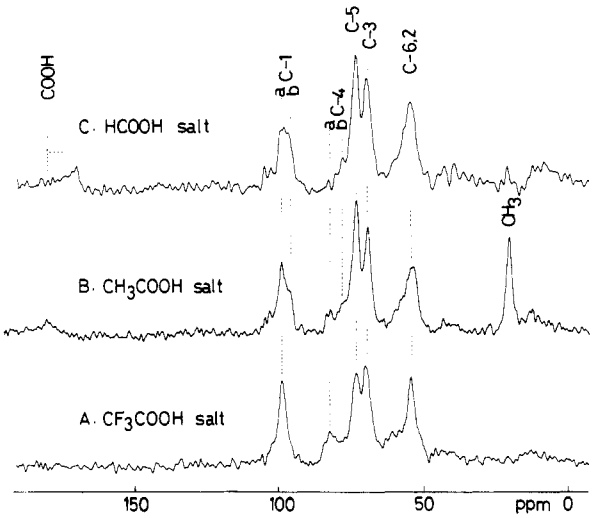

Figure 9. ^{13}C CP-MAS NMR spectra, 75.46 MHz, of chitosan salts with organic salts. (Note that there exist two types of salts in HCOOH and CH_3COOH salts.)

contain water molecules in the crystal.[3] The observation of the singlet peaks in the C-1 and C-4 ^{13}C NMR signals of these salts is thus consistent with the presence of the 2-fold helical conformation, in parallel with the interpretation of the ^{13}C NMR spectra of chitin (Figure 1A), the annealed chitosan described above (Figure 2), and the cellulose I form.[7,8,13]

Closer examination, however, shows that there exists a slight change in the C-1 ^{13}C NMR peak positions among several salts studied (Table IV). In particular, the C-1 ^{13}C NMR peak of HNO_3 salt resonates at the lowest position (at 101.1 ppm) and the corresponding peaks of $HClO_4$ and HBr salts are at 99.3–99.7 ppm, and the peak of HI salt resonates at the most shielded position (98.7 ppm). It appears that the relative peak positions of the C-1 ^{13}C NMR signals are in parallel with the lengths of the lattice parameter, c-axis (fiber axis), determined by X-ray diffraction, although these values are rather close to the limit of the experimental errors: 10.40 (HNO_3 salt), 10.42 (HBr salt), and 10.45 Å (HI salt).[3] This correlation may be reasonable, because the C-1 ^{13}C chemical shift is well related to the torsion angles at the glycosidic linkages.[4] Further analysis of the correlation between the ^{13}C chemical shifts and these torsion angles might be useful when detailed molecular parameters are determined in the future.

Table IV
^{13}C Chemical Shifts of Chitosan Salts in the Solid State (ppm from TMS)

acid	C-1	C-4	C-5	C-3	C-6	C-2
			Type I Salts with Inorganic Acids			
HNO_3	101.1 (97.4)[a]	85.1[b]	74.8	70.8	61.7	56.0
$HClO_4$	99.3	84.1	74.2	70.2	62.3	55.6
HBr	99.7 (96.8)[a]	85.1 (79.1)[a]	74.2	70.6	60.0	56.0
HI	98.7 (96.2)[a]	84.7 (78.9)[a]	73.8	70.0	61.3	55.6
			Type II Salts[c] with Inorganic Acids			
HCl	100.5, 96.8	79.4	74.4	71.2, 70.0	59.5, 58.1	55.2
H_2SO_4	100.3, 96.4	79.1	74.4	71.0, 69.8	59.8, 57.8	55.2
H_3PO_4	100.9, 96.6	79.5	74.4	70.8	59.2, 57.4	55.8
HIO_4	99.5, 97.3	78.4	74.4	70.6	58.4	55.8
			Salts with Organic Acids			
CF_3COOH	99.2[d]	82.9[d]	74.8	71.2	55.6[f]	
CH_3COOH	100.1[d,e] 97.3[e]	83.7,[d] 78.6[e]	74.6	71.0	55.4[f]	
HCOOH	100.1,[d,e] 97.3[e]	83.5,[d] 78.9[e]	74.4	70.6	56.2[f]	

[a] Minor peaks due to the presence of the type II form. [b] Shoulder peak at 87.1 ppm. [c] There remains a possibility that the other half of the C-4 doublet peak might be buried under the C-3 or C-5 peaks. [d] Type I salts. [e] Type II salts. [f] The C-6 and C-2 peaks are not resolved.

Type II Salts. The ^{13}C NMR spectra of the type II salts gave rise to larger splittings of peaks than those of the type I salts in the C-1 peaks (2.2–4.3 ppm) and the C-3 and C-6 to a lesser extent (1.4–2.0 ppm) (Figure 6A–C).[37] This trend is more noticeable in the ^{13}C NMR spectrum of the annealed sample of the HCl salt (Figure 6B). Previous X-ray fiber diagrams for the HCl salt of tendon chitosan revealed that annealing the salt improved its crystallinity without any crystalline modification,[3] in contrast to chitosan described above. The present powder samples of the HCl salts showed powder diagrams (Figure 5) coinciding with the previous fiber patterns.[38] In addition, there appears to be no contamination of the minor type I salts in the crystal of the inorganic type II salts. This observation may suggest that the conformation of the type II salts might be energetically more stabilized than that of the type I salts. This conclusion is not always true for the type II salts with organic acids, however.

In contrast to the type I salts, the ^{13}C NMR peak positions of the type II salts remained unchanged, within the experimental error (see Table II), among the variety of anions used. In other words, the conformations of these salts are almost identical for the several kinds examined. In this connection, it is noteworthy that the fiber X-ray patterns were much sharper at 100% humidity than those taken in vacuo, in which the *a* and *b* axes were decreased.[3] The amount of water molecules and their positions in the crystal have not yet been well determined but they depend on the size of anions.[3] In particular, the HF, HCl, and H_2SO_4 salts have similar crystal structures and anions are not arranged in regular positions in the crystals. It may be that there are cavities in the helices that can accommodate even the largest of these anions, and that variable amounts of water make the final adjustment, with more water compensating for smaller anions.[3]

The *c* axis of 40.73 Å corresponds to eight glucosamine residues.[3] Therefore, Ogawa and Inukai proposed either an 8-fold helix or a 4-fold helix of the dimer unit of glucosamine: the latter has different set of glycosidic torsion angles (ϕ, ψ) in the repeating unit. Obviously, the latter model of the four helices is more favorable for the interpretation of the significant splittings of the C-1, C-3, and C-6 (and C-4)[37] signals than the former. However, the possibility of the former, together with the presence of two independent chains, cannot be completely ruled out. In this case, it is likely that water molecules involved may have some role in modifying the conformation of one of the chains to some extent.

In conclusion, the present work clearly demonstrates that polymorphs of chitosan and two types of helical structures of its salts are readily distinguishable by ^{13}C NMR spectroscopy, as a complementary means to X-ray diffraction. In particular, additional information about nonequivalence of molecular conformations in polymorphs or other helical structures is easily available from examination of ^{13}C NMR spectra. For this reason, the combined use of ^{13}C NMR and X-ray is essential in analyzing the conformational features of various types of biological macromolecules such as polysaccharides.

Acknowledgment. We are grateful to Professor S. Hirano of Tottori University and Katokichi Co., Ltd., for providing us with chitosan samples from crab and shrimp shell, respectively. We thank Motoko Yokoi for her experimental assistance.

Registry No. Chitosan, 9012-76-4; chitosan·xHNO_3, 109744-45-8; chitosan·x$HClO_4$, 42617-21-0; chitosan·xHBr, 84861-60-9; chitosan·xHI, 108778-20-7; chitosan·xHCl, 70694-72-3; chitosan·xH_2SO_4, 72187-43-0; chitosan·xH_3PO_4, 109744-44-7; chitosan·xHIO_4, 109744-43-6; chitosan·xCF_3COOH, 109744-42-5; chitosan·xCH_3COOH, 87582-10-3; chitosan·xHCOOH, 66267-52-5.

References and Notes

(1) Muzarelli, R. A. A. *Chitin*; Pergamon: Oxford, 1977.
(2) Ogawa, K.; Oka, K.; Miyanishi, T.; Hirano, S. In *Chitin, Chitosan and Related Enzymes*; Zikakis, J. P., Ed.; Academic: Orlando, 1984; pp 327–345.
(3) Ogawa, K.; Inukai, S. *Carbohydr. Res.* **1987**, *160*, 425.
(4) Saitô, H. *Magn. Reson. Chem.* **1986**, *24*, 835.
(5) Saitô, H.; Izumi, G.; Mamizuka, T.; Suzuki, S.; Tabeta, R. *J. Chem. Soc., Chem. Commun.* **1982**, 1386.
(6) Saitô, H.; Izumi, G.; Tabeta, R. *Proc. NMR Symp., 21th* **1982**, 37–44.
(7) Atalla, R. H.; Gast, J. C.; Sindorf, D. W.; Bartuska, V. J.; Maciel, G. E. *J. Am. Chem. Soc.* **1980**, *102*, 3249.
(8) Earl, W. L.; VanderHart, D. L. *J. Am. Chem. Soc.* **1980**, *102*, 2351.
(9) Dudley, R. L.; Fyfe, C. A.; Stephenson, P. J.; Deslandes, Y.; Hammer, G. K.; Marchessault, R. H. *J. Am. Chem. Soc.* **1983**, *105*, 2469.
(10) Earl, W. L.; VanderHart, D. L. *Macromolecules* **1981**, *14*, 570.
(11) Atalla, R. H.; VanderHart, D. L. *Science (Washington, D.C.)* **1984**, *223*, 283.
(12) Maciel, G. E.; Kolodziejski, W. L.; Bertran, M. S.; Dale, B. E. *Macromolecules* **1982**, *15*, 686.
(13) Horii, F.; Hirai, A.; Kitamaru, R. *Polym. Bull.* **1982**, *8*, 163.
(14) Horii, F.; Hirai, A.; Kitamaru, R. *ACS Symp. Ser.* **1982**, *No. 260*, 27.
(15) Horii, F.; Hirai, A.; Kitamaru, R. *J. Carbohydr. Chem.* **1984**, *3*, 641.
(16) Saitô, H.; Tabeta, R.; Hirano, S. *Chem. Lett.* **1981**, 1479.
(17) Saitô, H.; Tabeta, R.; Hirano, S. In *Chitin and Chitosan. Proceedings of the Second International Conference on Chitin and Chitosan*; Hirano, S., Tokura, S., Eds.; Japanese Society of Chitin and Chitosan: Tottori, 1982; pp 71–76.
(18) Saitô, H.; Tabeta, R.; Harada, T. *Chem. Lett.* **1981**, 571.
(19) Fyfe, C. A.; Stephenson, P. J.; Taylor, M. G.; Bluhm, T. L.; Deslandes, Y.; Marchessault, R. H. *Macromolecules* **1984**, *17*, 501.
(20) Saitô, H.; Tabeta, R.; Sasaki, T.; Yoshioka, Y. *Bull. Chem. Soc. Jpn.* **1986**, *59*, 2093.
(21) Saitô, H.; Tabeta, R. *Chem. Lett.* **1981**, 713.
(22) Horii, F.; Hirai, A.; Kitamaru, R. *Macromolecules* **1986**, *19*, 930.
(23) Saitô, H.; Tabeta, R.; Shoji, A.; Ozaki, T.; Ando, I.; Asakura, T. In *Magnetic Resonance in Biology and Medicine*; Govil, G., Kheterapal, C. L., Saran, A., Eds.; Tata McGraw-Hill: New Delhi, 1985; pp 37–44.
(24) Ogawa, K.; Hirano, S.; Miyanishi, T.; Yui, T.; Watanabe, T. *Macromolecules* **1984**, *17*, 973.
(25) Clark, G. L.; Smith, A. F. *J. Phys. Chem.* **1937**, *40*, 863.
(26) Sakurai, K.; Shibano, T.; Kimura, K.; Takahashi, T. *Sen-i Gakkaishi* **1985**, *41*, T-361.
(27) Samuels, R. J. *J. Polym. Sci., Polym. Phys. Ed.* **1981**, *19*, 1081.
(28) Marchessault, R. H.; Sarko, A. *Adv. Carbohydr. Chem.* **1967**, *22*, 421.
(29) Pfeffer, P. E.; Parrish, F. W.; Unruh, J. *Carbohydr. Res.* **1980**, *84*, 13.
(30) Colson, P.; Jennings, J. H.; Smith, I. C. P. *J. Am. Chem. Soc.* **1974**, *96*, 8081.
(31) Darmon, S. E.; Rudall, K. M. *Discuss. Faraday Soc.* **1950**, 251.
(32) Averbach, B. L. Report of MITSG 75-17, National Technical Information Services, U. S. Department of Commerce, 1975.
(33) Shaefer, J.; Stejskal, E. O. In *Topics in ^{13}C NMR Spectroscopy*; Levy, G. C., Ed.; Wiley: New York, 1979; Vol. 3, pp 283–324.
(34) Sullivan, M. J.; Maciel, G. E. *Anal. Chem.* **1982**, *52*, 1615.
(35) Gidley, M. J.; Bociek, S. M. *J. Am. Chem. Soc.* **1985**, *107*, 7040.
(36) The HBr salt can take the type II conformation since the salt gave an X-ray fiber pattern corresponding to type II conformation when annealed in 80% isopropyl alcohol aqueous solution at 140 °C. However, there was no change in the fiber diagram of the HNO_3 salt even when annealed.
(37) The integrated peak intensities of the C-4 signals account for less than 50% of other single carbon signals. This finding suggests a possibility that the C-4 signal could be observed as a doublet and a "missing" pair of the upfield C-4 doublet peak might be buried underneath the C-5 or C-3 peak. As a piece of circumstantial evidence for this view, we noted that the C-4 signal of annealed poly(1→4)-α-D-galactosamine anhydride, which adopts a "kinked" 2-fold helix (Ogawa, K.; Tanaka, F.; Tamura, J.; Kadowaki, K.; Okamura, K. *Macromolecules* **1987**,

20, 1172), is split into a doublet peak (86.5 and 78.0 ppm) with a peak separation of 8.5 ppm (unpublished). At present, however, we assume the C-4 signal of the type II salt to be a singlet, unless new evidence is obtained.

(38) The lattice angles of the two peaks, 11.5° and 16.4°, are both a little larger than those observed at 100% relative humidity, 11.2° and 16.0°, respectively. These are equatorial reflections [the former is of (020) and (120) and the latter of (220) and (030) reflections, respectively] and change with relative humidity;[3] e.g., under vacuum, the former became 12.8. The present X-ray measurements were carried out at room humidity, ca. 40% relative humidity.

Complexation Chemistry of Sodium Borate with Poly(vinyl alcohol) and Small Diols. A ^{11}B NMR Study

Steve W. Sinton†

Exxon Production Research Company, Houston, Texas 77252-2189.
Received October 31, 1986

ABSTRACT: ^{11}B nuclear magnetic resonance spectroscopy was used to study the complexation chemistry of sodium borate (SB) with several organic polyols, including poly(vinyl alcohol) (PVA), in water. The cross-link structure in the PVA/SB system is deduced by comparison of diol/SB and PVA/SB spectra. Results are interpreted in terms of equilibrium constants, activation energies, and enthalpies for the various reactions involved. There are two ^{11}B signal components from PVA/SB solutions which can be assigned to cross-linking complexes. These two components are shown to have different spin relaxation rates. This behavior is discussed in terms of the mechanism for ^{11}B NMR relaxation and the polymer chain motions. Relationships between NMR parameters and viscosity in the PVA/SB system are discussed. It is concluded that certain theoretical descriptions of viscosity in associating polymer systems might be tested by combining mechanical and NMR measurements on the PVA/SB system.

Introduction

Sodium borate (SB) as common borax ($Na_2B_4O_7 \cdot 10H_2O$) at low concentrations in water dissociates completely into boric, $B(OH)_3$, and monoborate, $B(OH)_4^-$, molecules.[1] The acid/base equilibrium between these two species,

$$B(OH)_3 + H_2O \underset{k_{-1}}{\overset{k_1}{\rightleftharpoons}} B(OH)_4^- + H^+ \qquad (1)$$

has an equilibrium constant $pK_a = 9$.[2] In what follows, $B(OH)_3$ and $B(OH)_4^-$ are occasionally abbreviated as B and B^-, respectively. It has long been known that monoborate anions complex certain organic polyols according to eq 2 and 3.[3-10]

$$A + B^- \rightleftarrows AB^- + 2H_2O \qquad (2)$$

$$2A + B^- \rightleftarrows A_2B^- + 4H_2O \qquad (3)$$

In these equilibria the symbols A, AB^-, and A_2B^-, represent free polyol and polyol/monoborate complexes with 1:1 and 2:1 stoichiometry. For 1,3-type hydroxyl substitution on a linear hydrocarbon chain (e.g., poly(vinyl alcohol)) (PVA), complexation involves attachment of boron to adjacent oxygens, forming structures I and II for AB^- and A_2B^-, respectively.

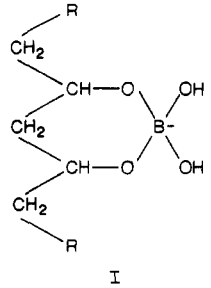

I

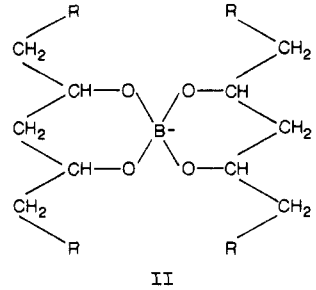

II

†Present address: Lockheed Missiles and Space Co., D/9350 B/204, 3251 Hanover St., Palo Alto, CA 94304.

Cross-linking caused by formation of 2:1 complexes has been cited as the chemical basis of enhanced viscosification in PVA/SB solutions.[11-14] Savins[11] attributed unusual rheological behavior of some PVA/SB compositions to a shear dependence in the formation of 2:1 complexes. Maerker and Sinton[14] extended this work to show that certain PVA/SB compositions result in shear-thickening and shear-thinning fluids. Shultz and Myers[12] calculated enthalpies for complexation from temperature-dependent dynamic mechanical data on borate-cross-linked PVA gels. Nickerson[13] argued from their results and his pH data that hydrogen bonding between polymer and monoborate anions and not 2:1 complexation must be responsible for viscosification and gelation effects in this system. More recently, the existence of PVA–borate complexes has been demonstrated with ^{11}B NMR.[14] NMR is a particularly useful technique because ^{11}B chemical shifts are sensitive to the oxygen symmetry (trigonal or tetrahedral) about boron[15,16] and to the size of polynuclear rings in 1:1 and 2:1 complexes.[8]

The work reported here was undertaken with two major goals in mind. First, it is desirable to fully characterize the complexation chemistry expressed by eq 1 and 2 and for this purpose a more thorough NMR study was performed. The second goal is to combine this chemical information with rheological data on PVA/SB solutions in order to develop a descriptive model of viscosity for such a solution. This paper is concerned primarily with the complexation chemistry while some results are discussed in terms of the relationship between chemistry and viscosity. The rheology of the PVA/SB system is covered in greater detail elsewhere.[11,12,14]

Several aspects of the complexation chemistry were studied in detail by using low-molecular-weight diols in addition to PVA. ^{11}B chemical shift assignments were easily made with these simple diols and were then useful for signal assignment in the PVA/SB case. A detailed picture of the chemistry involved in diol/SB systems was

0024-9297/87/2220-2430$01.50/0